Probing radiative neutrino mass models using trilepton channel at the LHC

Dounia Cherigui,[1,*] Chahrazed Guella,[1,†] Amine Ahriche,[2,3,4,‡] and Salah Nasri[5,6,§]

[1] *Faculté de Physique, Département de Génie Physique, Université des sciences et de la technologie, BP 1505, Oran, El M'Naouer, Algerie*

[2] *Department of Physics, University of Jijel, PB 98 Ouled Aissa, DZ-18000 Jijel, Algeria*

[3] *The Abdus Salam International Centre for Theoretical Physics, Strada Costiera 11, I-34014, Trieste, Italy.*

[4] *Department of Physics and Center for Theoretical Sciences, National Taiwan University, Taipei 106, Taiwan.*

[5] *Department of physics, United Arab Emirates University, P.O. Box 15551, Al-Ain, United Arab Emirates.*

[6] *Laboratoire de Physique Théorique, DZ-31000, Es-Senia University. Oran, Algeria.*

arXiv:1605.03640v2 [hep-ph] 30 Nov 2016

In this work, we probe a class of neutrino mass models through the lepton flavor violating interactions of a singlet charged scalar, $S^{\pm}$ at the LHC proton-proton collisions with 8 TeV and 14 TeV energies. This scalar couples to the leptons and induces many processes such as $pp \to \ell^{\pm}\ell^{\pm}\ell^{\mp} + \not{E}_T$. In our analysis we discuss the opposite sign same flavor leptons signal, as well as the background free channel with the tau contribution which can enhance the signal/background ratio for center of mass energies $\sqrt{s}$= 8 TeV and $\sqrt{s}$ = 14 TeV.

Keywords: Trilepton events, charged scalar, missing energy, LHC.

PACS: 04.50.Cd, 98.80.Cq, 11.30.Fs.

I. INTRODUCTION

There are number of motivations why the standard model (SM) of particle physics needs to be extended with new degrees of freedom. This includes the observation of neutrino oscillations for which the data can not be explained by massless neutrinos, the nature of dark matter (DM), and the origin of the matter-antimatter asymmetry of the universe.

One of the most popular mechanisms that generates small neutrino mass is the seesaw mechanism which comes in different types: type-I [1], the type-II [2, 3] and type-III [4]. This mechanism introduces new particles many orders of magnitude heavier than the electroweak scale that give rise to tiny neutrino mass after being integrated out from the low energy theory. To avoid fine tuning of the SM couplings, the mass scale of the new particles needs to be of order 10^{12} GeV which makes the high scale see-saw mechanism impossible to be test at laboratory experiments. In addition, for such superheavy mass scale the electroweak vacuum can be destabilized [5]. Other alternative realizations invoking 'low-scale mechanisms' were proposed in [6].

Another attractive way to induce naturally small neutrino mass is the radiative neutrino mass generation, where neutrino mass are generated at loop level [7–11]. Moreover, the scale of new physics is much smaller than in the conventional see-saw and can be of the same order as the electroweak scale for the three-loop radiative neutrino mass models. For instance, the KNT model proposed in [9] extends the SM with two singlet charged scalars, $S_{1,2}$, and one singlet fermion, N, all having masses around the TeV scale, making it testable at collider experiments. Different phenomenological aspects of this model, such as the DM relic density, were investigated in [12]. However, in order to match the neutrino mass and mixing with the experimental data without being in conflict with the bound on the process $\mu \to e + \gamma$, three generations of singlet fermions are required [13]. Generalization of the KNT model was proposed in [14] by promoting S_2 and N to multiplets of the $SU(2)_L$ gauge symmetry. In these models, the use of a

*Electronic address: dounia.cherigui@univ-usto.dz

†Electronic address: chahra.guella@gmail.com

‡Electronic address: aahriche@ictp.it

§Electronic address: snasri@uaeu.ac.ae

discrete symmetry that precludes the tree-level mass term for neutrinos allows the existence of a DM candidate which plays a role in the radiative neutrino mass generation and could also trigger the electroweak symmetry breaking [15].

Most of the neutrino mass motivated models, based either on radiative or seesaw mechanisms, contain charged scalar(s) whose interactions induce lepton flavor violating (LFV) processes, and thus their couplings are subject to severe experimental constraints [16, 17]. Probing these interactions is of great importance to identify through which mechanism neutrino mass is generated, and whether it is a Dirac or Majorana particle.

There has been many attempts to investigate different consequences of the new interactions in models motivated by neutrino mass at future colliders [18]. Ref. [19] investigated the possibility of testing the KNT model through the process $e^+ + e^- \to e^-\mu^+ + \not{E}_T$ at the ILC, where it was shown that it could be probed at ILC at center of mass energies 500 GeV and 1 TeV with and without the use of polarized beams. Similar study has been carried out for the processes $pp \to e^-e^+\,(\mu^-\mu^+, e^-\mu^+) + \not{E}_T$ through the production of the charged scalar $S^\pm$ via the Drell-Yan process and their decay modes which can give a detectable signal with two charged leptons and missing energy in the final state. The observation of an electron (positron) and anti-muon (muon) (the latter presents the most favorite channel), give us an indication for the signature of this class of model, where it has been shown that the LHC@14 TeV with 100 fb^{-1} luminosity can test this model [20].

In this work, without refering to a specific model of radiatively induced neutrino mass, we investigate the effect of the charged scalar $S^\pm$ on the trilepton final state ($\ell^\pm\ell^\pm\ell^\mp$) at the LHC, where the background consists of processes mediated by the gauge bosons $WZ(W\gamma^*)$ [21]. Then we will propose sets of benchmark points for different charged scalar masses and couplings which are consistent with LFV constraints and investigate the signal feasibility within the CMS analysis [22].

This paper is organized as follows. In section II, we describe the model and different experimental constraints. Then in section III, we use the 8 TeV LHC RUN-I data to put constraints on this class of models and probe the model at 14 TeV. In section IV, we consider two benchmark points and perform detailed analysis. Possible test of this class of models through a LFV background free process is investigated. Finally, we give our summary.

II. MODEL & SPACE PARAMETER

In this work, we consider a class of models that contain the following term in the Lagrangian [7, 9, 14, 15, 23]

$$\mathcal{L} \supset f_{\alpha\beta} L_\alpha^T C \epsilon L_\beta S^+ - m_S^2 S^+ S^- + \text{h.c.}, \tag{1}$$

where L_α is the left-handed lepton doublet, C is the charge conjugation operator, ϵ is the anti-symmetric tensor, $f_{\alpha\beta}$ are Yukawa couplings which are antisymmetric in the generation indices α and β, and $S^\pm$ is an $SU(2)_L$-singlet charged scalar field. The interactions above induce LFV processes such as $\mu \to e + \gamma$ and $\tau \to \mu + \gamma$, with branching fractions

$$\mathcal{B}(\mu \to e + \gamma) \simeq \frac{\alpha_{\rm em} \upsilon^4}{384\pi} \frac{|f^*_{\tau e} f_{\mu\tau}|^2}{m_S^4}, \tag{2}$$

$$\mathcal{B}(\tau \to \mu + \gamma) \simeq \frac{\alpha_{\rm em} \upsilon^4}{384\pi} \frac{|f^*_{\tau e} f_{\mu e}|^2}{m_S^4}, \tag{3}$$

where $\alpha_{\rm em}$ is the fine structure constant, and $\upsilon = 246$ GeV is the vacuum expectation value of the neutral component in the SM scalar doublet field. These two branching ratios must satisfy the experimental bounds $\mathcal{B}\,(\mu \to e + \gamma) < 5.7 \times 10^{-13}$ [16] and $\mathcal{B}\,(\tau \to \mu + \gamma) < 4.8 \times 10^{-8}$ [17]. Moreover, a new contribution to the muon's anomalous magnetic moment is induced at one-loop, given by

$$\delta a_\mu \sim \frac{m_\mu^2}{96\pi^2} \frac{|f_{e\mu}|^2 + |f_{\mu\tau}|^2}{m_S^2}. \tag{4}$$

The constraints on the LFV processes (2), (3) and (4), implies that $|f_{\alpha\beta}| \lesssim \varsigma m_S$, with ς is a dimensionful constant that depends on the experimental bounds. This means that the couplings f are suppressed for small values of the charged scalar mass.

Here, we consider the charged scalar mass in the range 100 GeV $< m_S <$ 2 TeV, while the couplings $f_{\alpha\beta}$ take random values that respect the above mentioned constraints (2), (3) and (4). These values are illustrated in Fig. 1, where we show the allowed space parameter for the charged scalar mass and couplings. It is worth mentioning that the couplings $f_{\alpha\beta}$ shown in Fig. 1 could match the observed neutrino oscillation values, and their values depend on the details of the models [13–15, 23][1]. Since our analysis is not restricted to a particular radiatively induced neutrino mass model, we present a scatter plot in Fig. 1-right for the combination $|f_{\alpha\rho}f_{\beta\rho}|^2$ which enter the expressions of the LFV observables. The large overlap between the region populated by the blue points in Fig. 1-left plot with the green is due to the fact that they get a common tau contribution in the expressions of the branching ratios in (2) and (3), whereas the red points correspond to larger values of $f_{e\mu}$ as compared to the two other combinations. Fig. 1-right shows the parameter space region for which upper experimental bounds of $\mathcal{B}(\mu \to e + \gamma)$ and $\mathcal{B}(\tau \to \mu + \gamma)$ are satisfied along the identified range of mass noting that this LFV bounds processes prompt m_S to large values once the corresponding coupling product $f_{\alpha\rho}f_{\beta\rho}$ becomes important.

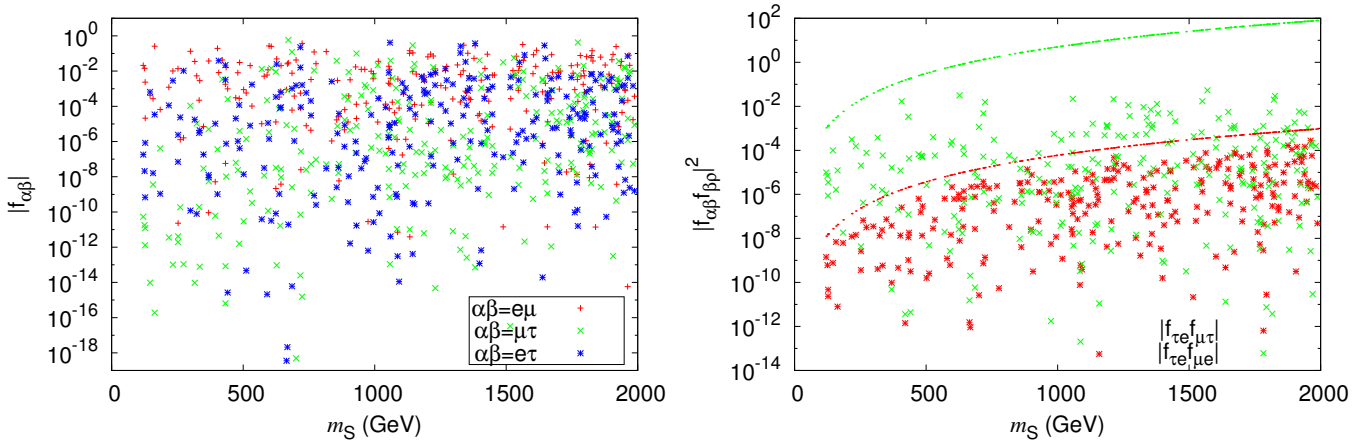

FIG. 1: The magnitude of f's versus m_S (left) and combination of the couplings versus m_S (right) with the experimental bounds $\mu \to e + \gamma$ and $\tau \to \mu + \gamma$ are represented by dashed lines.

III. CURRENT CONSTRAINTS ON TRILEPTON SIGNAL AT THE LHC

At the LHC, it is possible to produce a singly charged scalar associated with different sign different flavor charged leptons through W-boson exchange which at the parton level read as

$$q\bar{q}' \to W^{\pm} \to \ell^{\pm}\ell^{\pm}S^{*\mp} \to \ell^{\pm}\ell^{\pm}\ell^{\mp} + \not{E}_T, \tag{5}$$

where the charged scalar $S^{\pm}$ decays into charged lepton and neutrino giving rise to three leptons plus missing energy in the final state as shown in Fig. 2-a.

According to the diagram presented in Fig. 2-a, we have 7 contributions to this trilepton signal:

$$\ell\ell\ell \equiv ee\mu, e\mu\mu, ee\tau, e\tau\tau, \mu\mu\tau, \mu\tau\tau, e\mu\tau, \tag{6}$$

Here, the process that maximally violates the lepton flavor ($e\mu\tau$) has a small background, while the other six are accompanied by a large SM background. Such process with maximal LFV ($e\mu\tau$) can be a direct probe to the

[1] For example, the benchmark points values shown in Table I correspond to the model studied in [13], where the other model parameters (the couplings $g_{i\alpha}$ and the mass of the other charged scalar mass) are chosen in a way to match neutrino oscillation data, DM relic density and LFV constraints. For the models proposed in [14, 15], one can adjust the parameters so that most of the benchmark points shown in Fig. 1 fulfill the aforementioned constraints.

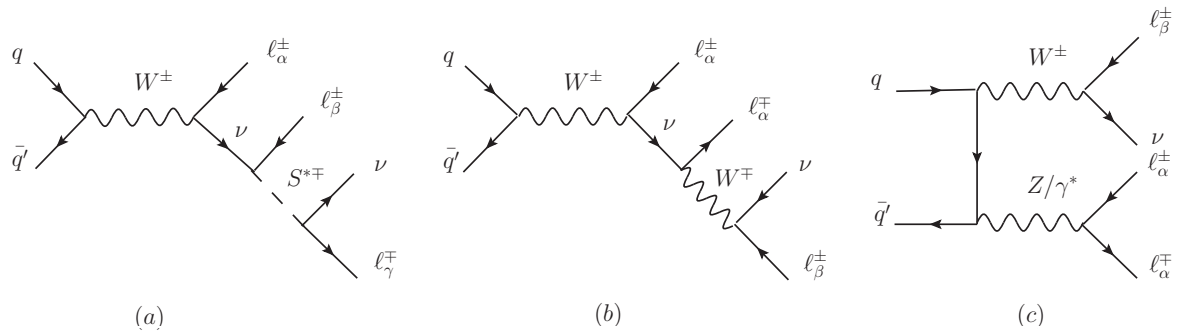

FIG. 2: Diagrams corresponding to the trilepton signal (a) and SM background (b,c).

interactions in (1). However, this process involves purely $S^\pm$mediated diagrams, and therefore has a very small cross section due to the smallness of the couplings $f_{\alpha\beta}$ and the heaviness of the charged scalars as dictated by the LFV constraints (2), (3) and (4). For the processes with the large SM background, such as $pp \to e^\pm e^\mp \mu^\pm + \not{E}_T$, the transverse missing energy receives two contributions $\not{E}_T \equiv \nu_\tau, \nu_\mu$. The process with $\not{E}_T \equiv \nu_\tau$ occurs only through purely S-mediated diagrams, and therefore has a suppressed cross section. However, the second process occurs through S-mediated and W/Z/γ-diagrams, and hence the cross section can be written as $\sigma_M = \sigma_{SM} + \sigma_S + \sigma_{interference}$. Therefore, the expected excess of events number could be either σ_S and/or $\sigma_{interference}$, where the former could be significant only when the charged scalar is on-shell. However we found that $\sigma_S/\sigma_{interference} < \mathcal{O}(10^{-5})$ for the benchmark points considered in our analysis. This leads us to confirm that the event number excess comes mainly from the interference contribution term.

Due to the difficulty in identifying the tau lepton at the LHC, we consider in our detailed analysis only the final state leptons $\ell = e, \mu$, where the missing energy $\not{E}_T$ can be any neutrino or antineutrino. The main process that contributes to the SM background for trilepton production is the irreducible background

$$q\bar{q}' \to W^\pm \to \ell^\pm \ell^\mp W^\pm \to \ell^\pm \ell^\pm \ell^\mp + \not{E}_T,\ q\bar{q}' \to ZW^\pm(\gamma^* W^\pm) \to \ell^\pm \ell^\pm \ell^\mp + \not{E}_T, \tag{7}$$

as shown in Fig. 2-b and -c. We use CalcHEP [24] to generate both the SM background events as well as the events from processes due to the extra interactions in (1) for CM energies $\sqrt{s} = 8$ TeV and 14 TeV. Here, the considered values of the $f_{\alpha\beta}$ Yukawa couplings and the charged scalar mass (m_S) make the branching ratios $\mathcal{B}(\mu \to e + \gamma)$ and $\mathcal{B}(\tau \to \mu + \gamma)$ just below the experimental bounds.

In our analysis, we look for the event number difference $N_{ex} = N_M - N_{BG}$, where N_M is the expected number of events number coming from both the new interactions and the SM processes, while N_{BG} is the background event number. Thus, with integrated luminosity $\mathcal{L}_{int}$, the excess of events is $N_{ex} = \mathcal{L}_{int}\,(\sigma_M - \sigma_{BG})$, and $N_{BG} = \mathcal{L}_{int}\sigma_{BG}$, with σ_{BG} and σ_M are the total cross sections due to interactions of the SM interactions and the one in Eq. (1), respectively, after imposing the selection cuts. Therefore the signal significance is given by

$$S = \frac{N_{ex}}{\sqrt{N_{ex} + N_{BG}}} = \frac{N_{ex}}{\sqrt{N_M}}. \tag{8}$$

One has to mention that the largest source of the SM background is the multi-jets events which can be misidentified as leptons in the detector. Among the dominant sources that give rise to these fake leptons we have the semileptonic decays of the charm and the bottom quark; and the photons conversion [25]. In order to reduce the contamination in the signal region, we require the electron events to have $p_T > 15$ GeV and $|\eta| < 2.5$, whereas all the muon candidates are required to have $p_T > 5$ GeV and $|\eta| < 2.4$. The hadronic decay of the tau charged lepton τ_{had} can be discriminated with $p_T > 15$ GeV and $|\eta| < 2.1$ [26]. Additional criteria can be applied in order to suppress the SM background coming from the QCD-multijet production [27].

In [22], the CMS collaboration presented a model-independent search for anomalous production of events with at least three isolated charged leptons using their data with an integrated luminosity of 19.5 fb^{-1} at $\sqrt{s} = 8$ TeV LHC. The analysis is based on the following criteria:

- The presence of at least three isolated leptons (muon, electron).
- The transverse momentum of muon and electron must satisfy $p_T^\ell > 10$ GeV.
- The pseudo-rapidity of leptons $|\eta^\ell| < 2.4$.
- The missing transverse energy $\not{E}_T < 50$ GeV.
- In order to remove the low-mass Drell-Yan processes as well as the 'Below-Z' and 'Above-Z' regions coming from background, the invariant mass of each opposite sign same flavor lepton pair must be in the range 75 GeV $< M_{\ell^+\ell^-} <$ 105 GeV.

Using these cuts, it has been found that a bound on the heavy-light neutrino mixing parameter ($|B_{lN}|^2$) for heavy neutrino masses up to 500 GeV can be established. For instance, $|B_{lN}|^2 < 2 \times 10^{-3}$ has been derived for $m_N \sim 100$ GeV [28].

In Fig. 3, we show the production cross section σ_M at the parton level for the first two processes in (6) as a function of the charged scalar mass for the benchmark points that are consistent with experimental bound on the LFV processes discussed in the previous section.

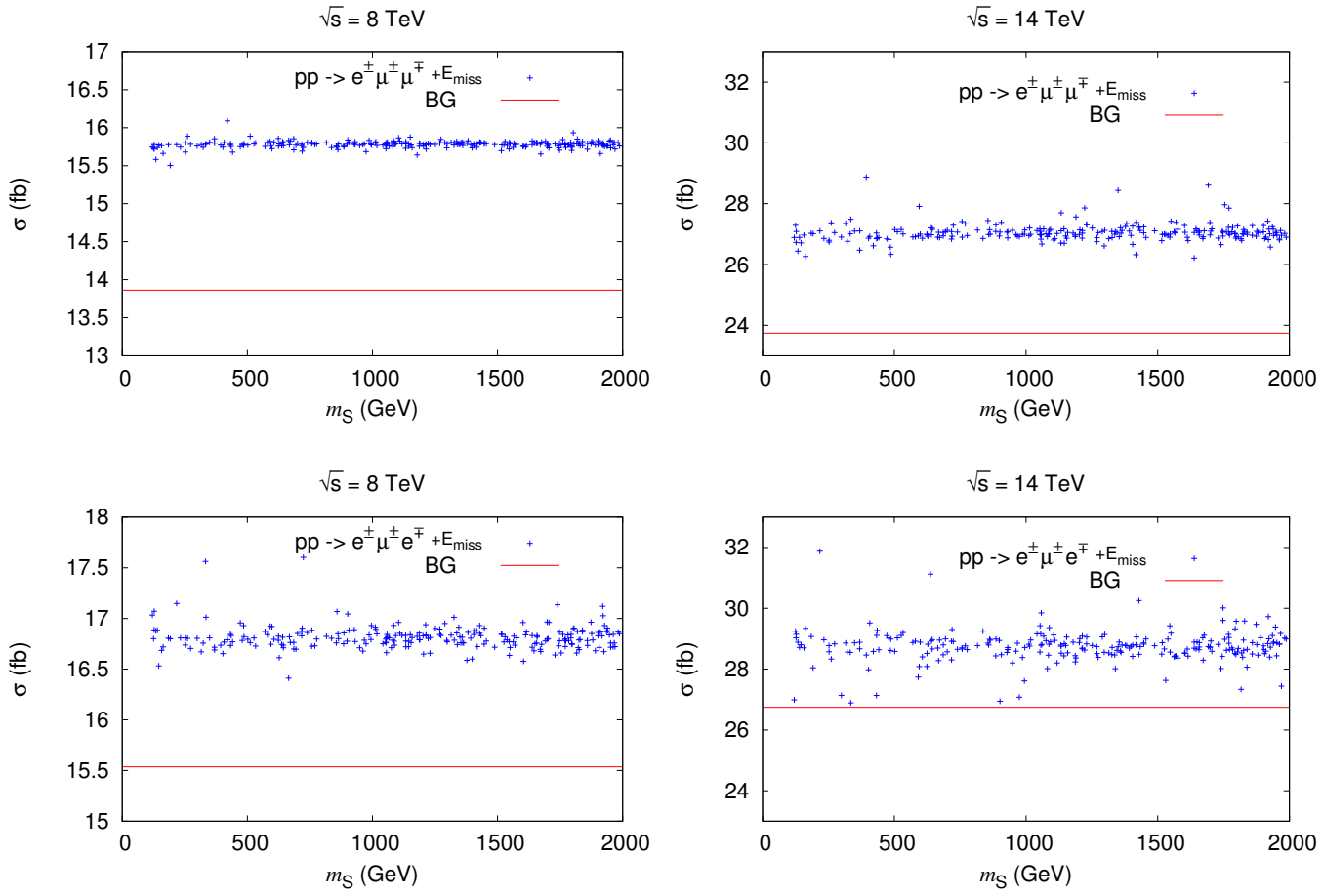

FIG. 3: The production cross section for the processes $pp \to e^\pm\mu^\pm\mu^\mp + \not{E}_T$ (top), $pp \to e^\pm\mu^\pm e^\mp + \not{E}_T$ (bottom) at $\sqrt{s} = 8$ TeV (left) and $\sqrt{s} = 14$ TeV (right) as function of charged scalar mass. The red lines correspond to the background cross section values.

We see that σ_M is larger than the one of the SM background σ_{BG} within the cuts used by the CMS collaboration, and increases with CM energy whereas it is essentially independent of the charged scalar mass. To see how important is the signal, we compute the significance taking into account the previous CMS cuts, for the two first processes in (6) for the set of benchmark points that fulfill the constraints on the LFV processes (2), (3) and (4) that are used previously in Fig. 1. After applying of the selection criteria quoted above, we show in Fig. 4 the significance for the

two considered channels at both 8 TeV and 14 TeV CM energy.

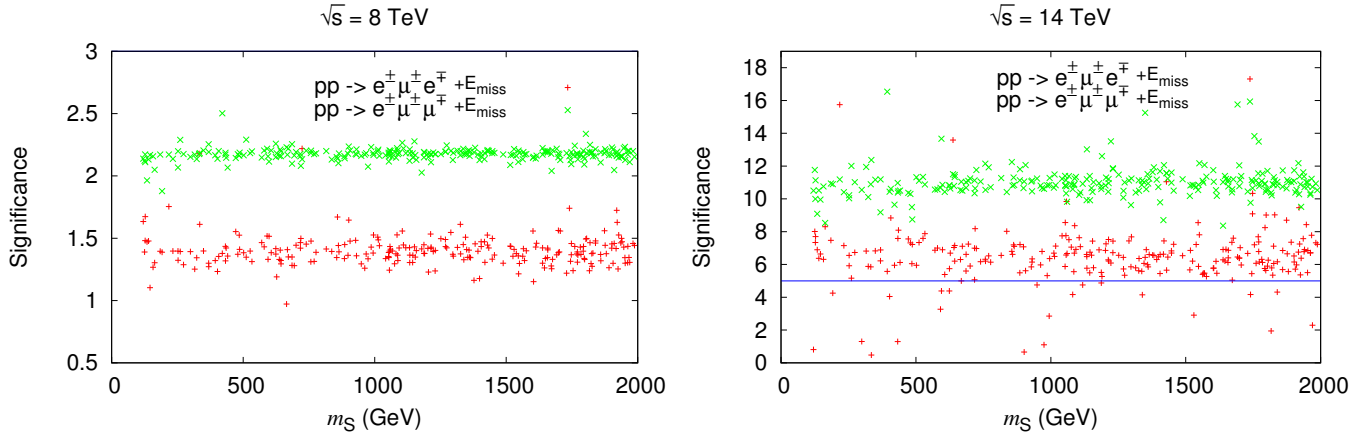

FIG. 4: The significance for the process $pp \to \ell^\pm\ell^\pm\ell^\mp + \not{E}_T$ at 8 TeV (left) and 14 TeV (right) versus the charged scalar mass for the integrated luminosity values 20.3 fb^{-1} and 100 fb^{-1}, respectively. The horizontal blue line indicates the significance value $S = 5$.

These results are consistent with searches for new phenomena in events with multilepton final states, they have not shown any significant deviation from SM expectations at 8 TeV CM energy. However, after imposing the same cuts at 14 TeV with 300 fb^{-1} of integrated luminosity, one shows that it is possible to get at least a 4 sigma excess for any benchmark point defined in Sec. II. Hence, we carry this study by searching a significant trilepton signal within this class of models at $\sqrt{s} = 8$ TeV and 14 TeV by choosing two benchmark points and look for different cuts where the significance could be larger.

IV. BENCHMARK ANALYSIS

In this section, we consider two benchmark points, denoted by B_1 and B_2, with the charged scalar masses 472 GeV and 1428 GeV (see Tab. I). Here, we first analyze the trilepton production with missing energy involving e and μ decay modes of the heavy charged scalar $S^\pm$ with $\sqrt{s} = 8$ TeV and 14 TeV. Then, we discuss possibility of observing the maximally LFV process signal $\ell^\pm\ell^\pm\ell^\mp \equiv e^\pm\mu^\pm\tau^\mp$.

A critical part in the analysis of signal events associated with new physics is the accurate estimation of the SM background. For this purpose, we study the event distributions for the SM background as well as the background plus the trilepton signal, and impose the cuts on the relevant observables as shown in Tab. II.

Point	m_S(GeV)	$f_{e\mu}$	$f_{e\tau}$	$f_{\mu\tau}$
B_1	472	$-(9.863 + i8.774) \times 10^{-2}$	$-(6.354 + i2.162) \times 10^{-2}$	$(0.78 + i1.375) \times 10^{-2}$
B_2	1428	$(5.646 + i549.32) \times 10^{-3}$	$-(2.265 + i1.237) \times 10^{-1}$	$-(0.41 - i3.58) \times 10^{-2}$

TABLE I: Two benchmark points selected from the allowed parameter space of the model.

We note that the imposed cut values on the kinematic variables are different than those provided by CMS, except for the range of the invariant mass of two charged leptons $M_{\ell^+\ell^-}$, and the pseudo rapidity η^ℓ which still relevant for discriminating the signal from background. Moreover, we attempt to introduce supplementary criteria by applying cuts on the invariant masses $M_{e^+\mu^+}$ and $M_{\ell,\nu}$ of the fermion pairs $(e^+\mu^+)$ and (ℓ, ν), respectively. These extra cuts allowed us to optimize the total cross section for the signal at $\sqrt{s} = 8$ TeV and 14 TeV. This is illustrated in Fig. 5 where we present the angular distribution between pairs of leptons, the energy distribution of lepton, and the invariant mass distribution of the three leptons at $\sqrt{s} = 14$ TeV.

$e^{\pm}\mu^{\pm}e^{\mp}+\not{E}_T$ @ 8 TeV	$e^{\pm}\mu^{\pm}e^{\mp}+\not{E}_T$ @ 14 TeV	$e^{\pm}\mu^{\pm}\mu^{\mp}+\not{E}_T$ @ 8 TeV	$e^{\pm}\mu^{\pm}\mu^{\mp}+\not{E}_T$ @ 14 TeV
$70 < M_{e^-e^+} < 110$	$70 < M_{e^-e^+} < 110$	$80 < M_{\mu^-\mu^+} < 100$	$80 < M_{\mu^-\mu^+} < 110$
$M_{e^+\mu^+} < 200$	$M_{e^+\mu^+} < 230$	$M_{e^+\mu^+} < 200$	$M_{e^+\mu^+} < 230$
$M_{e^-\nu} < 206$	$M_{e^-\nu} < 220$	$M_{\mu^-\nu} < 185$	$M_{\mu^-\nu} < 245$
$10 < p_T^{\ell} < 100$	$10 < p_T^{\ell} < 90$	$10 < p_T^{\ell} < 100$	$10 < p_T^{\ell} < 130$
$\lvert\eta^{\ell}\rvert < 3$	$\lvert\eta^{\ell}\rvert < 3$	$\lvert\eta^{\ell}\rvert < 3$	$\lvert\eta^{\ell}\rvert < 3$
$\not{E}_T < 100$	$\not{E}_T < 90$	$\not{E}_T < 120$	$\not{E}_T < 90$

TABLE II: Applied cuts on different kinematical variables: $M_{\ell\ell}$ (invariant mass), p_T^{ℓ} (charged lepton transverse momentum), $\not{E}_T$ (transverse missing energy), and η^{ℓ} (pseudo-rapidity). The energy dimension variables are in GeV unit.

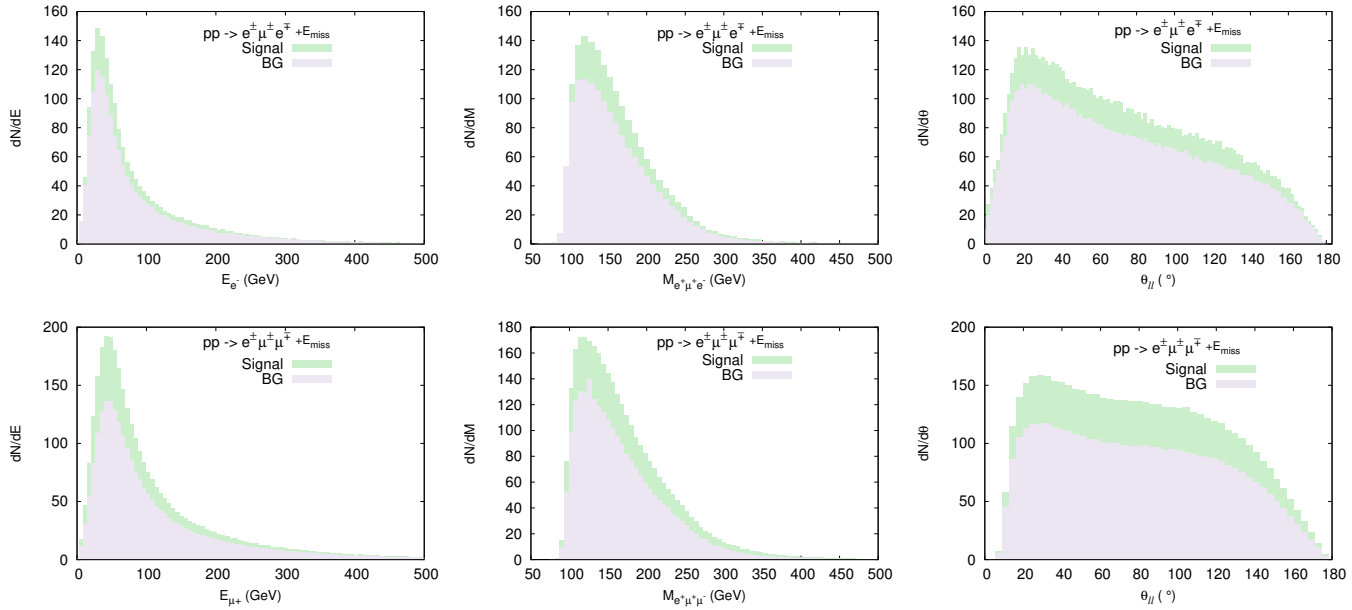

FIG. 5: Number of events of the energy distribution E_{ℓ}, the invariant mass distribution of the three leptons $M_{\ell\ell\ell}$, and the angular distribution between pairs of leptons $\theta_{\ell\ell}$ at $\sqrt{s} = 14$ TeV and $\int \mathcal{L}dt = 300\ fb^{-1}$.

The kinematical distributions in Fig. 5 show a significant excess of events which is an indication of a trilepton signal. Clearly, there is a larger excess in the channel $e\mu\mu$ than in the $ee\mu$ channel for this benchmark. According to the cross section values in Fig. 3, we expect the same difference for other benchmarks. The overall shape of the distributions for the signal and the background looks very similar due to two reasons: (1) the source of the event excess is the interference contribution $\sigma_{interference}$, and (2) the cuts are chosen such that the difference $d\left(\sigma_M - \sigma_{BG}\right)/dX$ is strictly positive, where X represents the kinematic variables in Tab. II. In Tab. III, we present the cross section values of the signal and background after imposing the cuts for the CM energies 8 TeV and 14 TeV. The corresponding significance for each benchmark point is shown in Tab. IV.

Process	B_1@8 TeV	B_2@8 TeV	B_1@14 TeV	B_2@14 TeV
$\sigma_{BG}\left(e^{\pm}\mu^{\pm}e^{\mp}+\not{E}_T\right)$	22.79		40.84	
$\sigma_{BG}\left(e^{\pm}\mu^{\pm}\mu^{\mp}+\not{E}_T\right)$	20.74		46.44	
$\sigma_{EX}\left(e^{\pm}\mu^{\pm}e^{\mp}+\not{E}_T\right)$	28.12	28.06	49.70	48.55
$\sigma_{EX}\left(e^{\pm}\mu^{\pm}\mu^{\mp}+\not{E}_T\right)$	26.13	26.06	57.28	56.80

TABLE III: The expected and background cross section values (in fb) at 8 TeVand 14 TeV for the two benchmark points B_1 and B_2.

Process	Benchmark	$N_{20.3}$	$S_{20.3}$	N_{300}	S_{300}
$pp \to e^{\pm}\mu^{\pm}e^{\mp} + \not{E}_T$	B_1	108.20	4.53	2058	21.77
	B_2	106.98	4.48	2313	19.16
$pp \to e^{\pm}\mu^{\pm}\mu^{\mp} + \not{E}_T$	B_1	109.42	4.75	3252	24.81
	B_2	108.02	4.69	3108	23.81

TABLE IV: The significance corresponding to the integrated luminosity values $\mathcal{L}_{int} = 20.3$ (300) fb^{-1} at 8 TeV (14 TeV) for the benchmark points B_1 and B_2.

In order to see how does the significance change with large charged scalar mass values, we consider the benchmark point B_1 given in Tab. I, and increase m_S at both CM energies 8 TeV and 14 TeV for the integrated luminosity 20.3 fb^{-1} and 300 fb^{-1}, respectively. We first keep the couplings $f_{\alpha\beta}$ to be constant and therefore the LFV constraints get relaxed with larger m_S values. In the second case, we vary m_S values while keeping LFV observables, such as $B(\ell_\alpha \to \ell_\beta + \gamma)$, constant. The two cases are shown in Fig. 6 with dashed and solid lines, respectively. Thus, whatever the values of charged scalar mass or the LFV branching ratios, the significance should lie in between these two curves. We can see from the figure that the significance can reach 3σ for any charged scalar $S^{\pm}$ mass under 2 TeV, and 5σ is ensured until $m_S = 3$ TeV in the case where $\sqrt{s} = 14$ TeV.

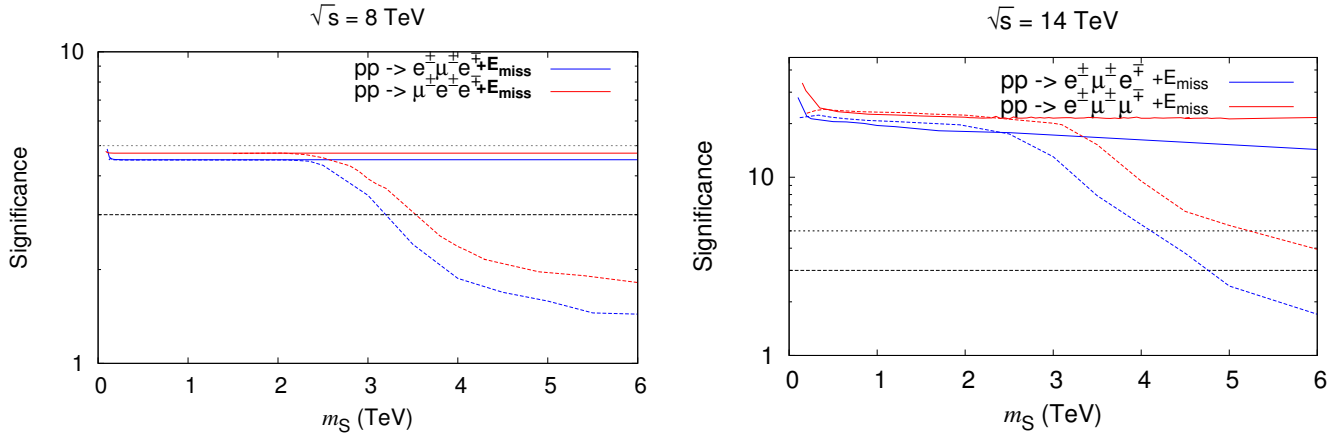

FIG. 6: Significance for the relevant process $pp \to \ell^{\pm}\ell^{\pm}\ell^{\mp} + \not{E}_T$ at $\sqrt{s} = 8$ TeV (left) and $\sqrt{s} = 14$ TeV (right) within the new cuts. The black dashed horizontal lines represent the significance value $S = 3$, 5, respectively. solid and the dashed lines are explained in the text.

We remark here that the Feynman diagrams that mediate the processes $pp \to \ell^{\pm}\ell^{\pm}\ell^{\mp} + \not{E}_T$ can be classified as SM and non-SM diagrams with amplitudes $\mathcal{M}_{SM}$ and $\mathcal{M}_S$, respectively. Therefore, the event number difference $N_{ex} = N_M - N_{BG}$ is proportional to the combination $\sigma_{interference} \propto Re\left(\mathcal{M}^{\dagger}_{SM}\mathcal{M}_S\right)$, since σ_S is negligible as mentioned previously. In other words, the significance shown in Fig. 6 is directly proportional to the couplings combination $|f_{\alpha\rho}f_{\beta\rho}|^2$ that appears in the expressions of the branching ratios of the processes $\mu \to e + \gamma$ and $\tau \to \mu + \gamma$. This means that there is a direct correlation between the discovery of the LFV processes and the signals.

In our analysis at $\sqrt{s} = 14$ TeV, we have presented the points which can be discovered with an integrated luminosity of 300 fb^{-1}. However, another way to probe the interaction (1) is to extend our analysis by considering a maximally LFV process like the process $pp \to e^{\pm}\mu^{\pm}\tau^{\mp} + \not{E}_T$, where the tau lepton can be identified through its hadronic decay [29] rather than its leptonic one in order to avoid an additional source of missing energy. In addition to the case of $\sqrt{s} = 14$ TeV, we consider also the very high energy such as at the HL-LHC $\sqrt{s} = 100$ TeV. Then, the event number here is given by

$$N_{e\mu\tau} = L \times \sigma(pp \to e^{\pm}\mu^{\pm}\tau^{\mp} + \not{E}_T)\mathcal{B}(\tau \to hadrons), \tag{9}$$

where the corresponding background event number is given by

$$N_{BG} = L \times \sigma(pp \to WWW)\mathcal{B}(W \to e\nu)\mathcal{B}(W \to \mu\nu)\mathcal{B}(W \to \tau\nu)\mathcal{B}(\tau \to hadrons). \quad (10)$$

We find that the significance is so small at both $\sqrt{s}$ =14 TeV and 100 TeV for luminosity values of the order $\mathcal{O}(\text{ab}^{-1})$. Detailed investigation is required to reach final conclusion about the possibility of detecting the maximally LFV in this model (1).

V. SUMMARY

In this paper, we investigate the effect of a singlet charged scalar at the LHC by performing a detailed analysis of three isolated leptons in the final state. First we applied the same cuts used by the CMS collaboration at 8 TeV on a large number of benchmarks that are consistent with LFV bounds and we found no significant deviation from the SM. Whereas, within the same cuts we expect significant deviation at 14 TeV. So to enhance the signal over the background, we applied new cuts for both 8 TeV and 14 TeV. We have chosen two benchmark points B_1 and B_2 with different values of m_S in order to probe the effect of this charged scalar in the tripleton channel and we found that a deviation from the SM can be seen using 8 TeV data and expect that a discovery is potentially possible at 14 TeV. Using our analysis of 8 TeV (14 TeV), we can exclude charged scalar masses $m_S <$ 3 TeV ($m_S <$ 4 TeV). We found that the significance is directly proportional to $\mathcal{B}(\ell_\alpha \to \ell_\beta + \gamma)$, and hence there is a direct correlation between the LFV discovery and our signal.

Another way to search for the trilepton signal is via the maximally LFV processes such $e^\pm\mu^\pm\tau^\mp$, where the tau lepton is identified through its hadronic decay. However, even at $\sqrt{s}$ = 100 TeV the significance is too small for luminosity values of the order $\mathcal{O}(ab^{-1})$.

Acknowledgments

We would like to thank C.-S. Chen and J.M. No for useful discussion; and A.B. Hammou for valuable comments on the manuscript. C.G. and D.C. would like to thank the ICTP for the warm hospitality during part of this work. A.A. is supported by the Algerian Ministry of Higher Education and Scientific Research under the CNEPRU Project No B00L02UN180120140040.

[1] P. Minkowski, Phys. Lett. B 67, 421 (1977); M. Gell-Mann, P. Ramond and R. Slansky, Proceedings of the Supergravity Stony Brook Workshop, New York 1979, eds. P. Van Nieuwenhuizen and D. Freedman; T. Yanagida, Proceedings of the Workshop on Unified Theories and Baryon Number in the Universe, Tsukuba, Japan 1979, eds. A. Sawada and A. Sugamoto; R. N. Mohapatra and G. Senjanovic, Phys. Rev. Lett. 44, 912 (1980).

[2] J. Schechter and J.W.F. Valle, Phys. Rev. D 22, 2227 (1980).

[3] T. P. Cheng and L. F. Li, Phys. Rev. D**22** (1980) 2860; M. Magg and C. Wetterich, Phys. Lett. B**94** (1980) 61; C. Wetterich, Nucl. Phys. B**187** (1981) 343; R. N. Mohapatra and G. Senjanovic, Phys. Rev. D**23** (1981) 165.

[4] R. Foot, H. Lew, X. G. He and G. C. Joshi, Z. Phys. C**44** (1989) 441.

[5] A. de Gouvea, D. Hernandez and T. M. P. Tait, Phys. Rev. D**89**, no. 11, 115005 (2014).

[6] S. M. Boucenna, S. Morisi and J. W. F. Valle, Adv. High Energy Phys. **2014**, 831598 (2014) [arXiv:1404.3751 [hep-ph]]; F. Borzumati and Y. Nomura, Phys. Rev. D**64** (2001) 053005 [hep-ph/0007018]; M. Fabbrichesi and S. T. Petcov, Eur. Phys. J. C**74** (2014) 2774 [arXiv:1304.4001 [hep-ph]]; P. H. Gu, M. Hirsch, U. Sarkar and J. W. F. Valle, Phys. Rev. D**79** (2009) 033010 [arXiv:0811.0953 [hep-ph]]; P. Fileviez Perez, T. Han and T. Li, Phys. Rev. D**80** (2009) 073015 [arXiv:0907.4186 [hep-ph]]; E. Ma, Mod. Phys. Lett. A**24** (2009) 2491 [arXiv:0905.2972 [hep-ph]]; A. Ahriche, S. M. Boucenna and S. Nasri, Phys. Rev. D**93** (2016) no.7, 075036 [arXiv:1601.04336 [hep-ph]].

[7] A. Zee, Phys. Lett. B 161, 141 (1985); A. Zee, Nucl. Phys. B 264, 99 (1986); K.S. Babu, Phys. Lett. B 203, 132 (1988).

[8] E. Ma, Phys. Rev. Lett. **81**(1998) 1171 [hep-ph/9805219].

[9] L. M. Krauss, S. Nasri and M. Trodden, Phys. Rev. D**67**, 085002 (2003) [hep-ph/0210389].

[10] M. Aoki, S. Kanemura and O. Seto, Phys. Rev. Lett. 102, 051805 (2009) [arXiv:0807.0361 [hep-ph]]; M. Aoki, S. Kanemura and O. Seto, Phys. Rev. D 80 (2009) 033007 [arXiv:0904.3829 [hep-ph]].

[11] H. Okada and K. Yagyu, Phys. Lett. B**756** (2016) 337 [arXiv:1601.05038 [hep-ph]]. Y. Farzan, JHEP **1505** (2015) 029 [arXiv:1412.6283 [hep-ph]]. D. Aristizabal Sierra, A. Degee, L. Dorame and M. Hirsch, JHEP **1503** (2015) 040 [arXiv:1411.7038 [hep-ph]]. Y. Farzan, S. Pascoli and M. A. Schmidt, JHEP **1303** (2013) 107 [arXiv:1208.2732 [hep-ph]]. Y. Farzan and E. Ma, Phys. Rev. D **86** (2012) 033007 [arXiv:1204.4890 [hep-ph]]. Y. Farzan, S. Pascoli and M. A. Schmidt, JHEP **1010** (2010) 111 [arXiv:1005.5323 [hep-ph]]. Y. Farzan, Phys. Rev. D **80** (2009) 073009 [arXiv:0908.3729 [hep-ph]]. C. Boehm, Y. Farzan, T. Hambye, S. Palomares-Ruiz and S. Pascoli, Phys. Rev. D **77** (2008) 043516 [hep-ph/0612228]. D. Restrepo, O. Zapata and C. E. Yaguna, JHEP **1311** (2013) 011 [arXiv:1308.3655 [hep-ph]]. P. W. Angel, Y. Cai, N. L. Rodd, M. A. Schmidt and R. R. Volkas, JHEP **1310** (2013) 118 Erratum: [JHEP **1411** (2014) 092] [arXiv:1308.0463 [hep-ph]].

[12] K. Cheung and O. Seto, Phys. Rev. D**69**, 113009 (2004) [hep-ph/0403003]; A. Ahriche, K. L. McDonald and S. Nasri, Phys. Rev. D **92**, no. 9, 095020 (2015) [arXiv:1508.05881].

[13] A. Ahriche and S. Nasri, JCAP**1307**, 035 (2013) [arXiv:1304.2055]; E. A. Baltz and L. Bergstrom, Phys. Rev. D**67**, 043516 (2003) [hep-ph/0211325].

[14] A. Ahriche, C. S. Chen, K. L. McDonald and S. Nasri, Phys. Rev. D**90**, 015024 (2014) [arXiv:1404.2696 [hep-ph]]; A. Ahriche, K. L. McDonald and S. Nasri, JHEP**1410**, 167 (2014) [arXiv:1404.5917 [hep-ph]]; A. Ahriche, K. L. McDonald, S. Nasri and T. Toma, Phys. Lett. B**746**, 430 (2015) [arXiv:1504.05755 [hep-ph]].

[15] A. Ahriche, K. L. McDonald and S. Nasri, JHEP**1602**, 038 (2016) [arXiv:1404.5917 [hep-ph]].

[16] J. Adam *et al.* [MEG Collaboration], Phys. Rev. Lett.**110** (2013) 201801 [arXiv:1303.0754 [hep-ex]].

[17] K. A. Olive *et al.* [Particle Data Group Collaboration], "Review of Particle Physics,"Chin. Phys. C**38**, 090001 (2014).

[18] W. Y. Keung and G. Senjanovic, Phys. Rev. Lett. **50**, 1427 (1983); P. Fileviez Perez, T. Han, G. Y. Huang, T. Li and K. Wang, Phys. Rev. D**78**, 071301 (2008) [arXiv:0803.3450 [hep-ph]]; S. Gabriel, B. Mukhopadhyaya, S. Nandi and S. K. Rai, Phys. Lett. B**669**, 180 (2008) [arXiv:0804.1112 [hep-ph]]; C. S. Chen, C. Q. Geng, J. N. Ng and J. M. S. Wu, JHEP**0708**, 022 (2007) [arXiv:0706.1964 [hep-ph]]; J. Kersten and A. Y. Smirnov, Phys. Rev. D**76**, 073005 (2007) [arXiv:0705.3221 [hep-ph]]; A. Das and N. Okada, Phys. Rev. D**88**, 113001 (2013) [arXiv:1207.3734 [hep-ph]]; D. Atwood, S. Bar-Shalom and A. Soni, Phys. Rev. D**76**, 033004 (2007) [hep-ph/0701005]; S. Kanemura, T. Nabeshima and H. Sugiyama, Phys. Rev. D**87**, no. 1, 015009 (2013) [arXiv:1207.7061 [hep-ph]]; P. S. B. Dev and A. Pilaftsis, Phys. Rev. D**86**, 113001 (2012) [arXiv:1209.4051 [hep-ph]]; S. Antusch and O. Fischer, JHEP **1410**, 094 (2014) [arXiv:1407.6607 [hep-ph]]; S. Antusch, E. Cazzato and O. Fischer, JHEP**1604**, 189 (2016) [arXiv:1512.06035 [hep-ph]]; S. Antusch, E. Cazzato and O. Fischer, arXiv:1604.02420 [hep-ph].

[19] A. Ahriche, S. Nasri and R. Soualah, Phys. Rev. D**89**, 095010 (2014) [arXiv:1403.5694 [hep-ph]].

[20] C. Guella, D. Cherigui, A. Ahriche, S. Nasri and R. Soualah, Phys. Rev. D **93** (2016) no.9, 095022 [arXiv:1601.04342 [hep-ph]]; A. Pilaftsis, Z. Phys. C**55**, 275 (1992) [hep-ph/9901206].

[21] A. Das, N. Nagata and N. Okada, JHEP**1603**, 049 (2016) [arXiv:1601.05079 [hep-ph]]; A. Chatterjee, N. Chakrabarty and B. Mukhopadhyaya, Phys. Lett. B**754**, 14 (2016).

[22] S. Chatrchyan *et al.* [CMS Collaboration], Phys. Rev. D **90** (2014) 032006 [arXiv:1404.5801 [hep-ex]]. For an earlier analysis with $\sqrt{s} = 7$ TeV LHC data, see S. Chatrchyan et al. [CMS Collaboration], JHEP 1206, 169 (2012) [arXiv:1204.5341 [hep-ex]].

[23] For example: K. S. Babu and C. Macesanu, Phys. Rev. D**67** (2003) 073010 [hep-ph/0212058].; S. Kanemura, T. Nabeshima and H. Sugiyama, Phys. Lett. B**703** (2011) 66 [arXiv:1106.2480 [hep-ph]]; M. Lindner, D. Schmidt and T. Schwetz, Phys. Lett. B**705** (2011) 324 [arXiv:1105.4626 [hep-ph]]; S. S. C. Law and K. L. McDonald, Int. J. Mod. Phys. A**29** (2014) 1450064 [arXiv:1303.6384 [hep-ph]]; C. S. Chen, C. Q. Geng and D. V. Zhuridov, arXiv:0806.2698 [hep-ph]; K. Nishiwaki, H. Okada and Y. Orikasa, Phys. Rev. D**92** (2015) no.9, 093013 [arXiv:1507.02412 [hep-ph]]; T. Nomura, H. Okada and Y. Orikasa, Phys. Rev. D**93** (2016) no.11, 113008 [arXiv:1603.04631 [hep-ph]]; T. Nomura, H. Okada and Y. Orikasa, arXiv:1602.08302 [hep-ph].

[24] A. Belyaev, N. D. Christensen and A. Pukhov, Comput. Phys. Commun. **184**, 1729 (2013) [arXiv:1207.6082 [hep-ph]].

[25] [CMS Collaboration], CMS-PAS-MUO-10-002.

[26] S. Chatrchyan *et al.* [CMS Collaboration], Eur. Phys. J. C**72**, 2189 (2012) [arXiv:1207.2666 [hep-ex]].

[27] [CMS Collaboration], CMS-PAS-EGM-10-004.

[28] A. Das, P. S. Bhupal Dev and N. Okada, Phys. Lett. B**735**, 364 (2014) [arXiv:1405.0177 [hep-ph]]; A. Das and N. Okada, Phys. Rev. D**93** (2016) 033003 [arXiv:1510.04790 [hep-ph]].

[29] A. J. Weinstein, Nucl. Phys. Proc. Suppl.**76**, 497 (1999) [hep-ex/9811044].